AIAA JOURNAL
Vol. 34, No. 6, June 1996

Spatial Transformation of the Discrete Sound Field from a Propeller

X. D. Li* and S. Zhou†
Beijing University of Aeronautics and Astronautics, Beijing 100083, People's Republic of China

A technique for the spatial transformation of the discrete sound field from a propeller is proposed that is based on solving the Ffowcs Williams and Hawkings equation with quadrupole source term neglected. Since the blade surface velocity is fully specified, numerical inversion of Farassat's integral is used to relate the blade surface pressures to the finite number of measurements in the acoustic field. With the reconstructed aerodynamic loading, the whole sound field is naturally predicted using Farassat's integral. Since the inverse problem is ill posed, the Tikhonov regularization method is used to stabilize the solution. The optimal regularization parameter is chosen by generalized cross-validation criterion. Numerical results show that the reconstruction is inaccurate in the presence of measurement noise (error) but the spatial transformation of discrete sound filed remains satisfactory.

Nomenclature

A	= model matrix
$\boldsymbol{b}$	= observer data
$\bar{\boldsymbol{b}}$	= error-free component of observer data
c_0	= speed of sound
c_p	= pressure coefficient
$\boldsymbol{e}$	= perturbation errors
$f(\bar{\boldsymbol{x}}, t)$	= description of body surface, $f > 0$ outside the body
$\boldsymbol{I}$	= identity matrix
K_p	= kernel due to source loading
K_{v_n}	= kernel due to source thickness
l_i	= force per unit area on the fluid
M	= local Mach number based on c_0
M_n	= local Mach number in normal direction, $M \cdot \hat{\boldsymbol{n}}$
M_r	= local Mach number in propagation direction, $M \cdot \hat{\boldsymbol{r}}$
$\dot{M}_r$	= derivative of Mach number in propagation direction, $(\partial M/\partial r) \cdot \hat{\boldsymbol{r}}$
$\hat{\boldsymbol{n}}$	= unit outward normal to $f = 0$
p	= surface pressure $p_a - p_0$ on $f = 0$, p_a = absolute surface pressure, and p_0 = ambient pressure in the undisturbed medium
p'	= acoustic pressure
p'_L, p'_T	= loading and thickness acoustic pressure
$[p'(\bar{\boldsymbol{x}}, t)]_d$	= exact acoustic pressures
$[p'(\bar{\boldsymbol{x}}, t)]_m$	= acoustic pressures contaminated by additive noise
$\boldsymbol{R}$	= resolution matrix in model space, $\boldsymbol{R}_{\text{tr}}$ = trace of $\boldsymbol{R}$
$\boldsymbol{r}$	= $\bar{\boldsymbol{x}} - \boldsymbol{y}$, $r = \lvert\bar{\boldsymbol{x}} - \boldsymbol{y}\rvert$
$\hat{\boldsymbol{r}}$	= unit radiation vector, $\boldsymbol{r}/r$
ret	= expression is evaluated at retarded time, $\tau = t - r/c_0$
S	= element of blade surface area (in dS)
S/N	= signal-to-noise ratio
T	= period of acoustic pressure
t	= observer time
U	= $m \times m$ unitary matrix composed of the eigenvectors of (AA^T)
$\boldsymbol{u}_i^T$	= transposed left singular vectors of A, $U = (\boldsymbol{u}_1, \ldots, \boldsymbol{u}_m)$
$v_n(\bar{\boldsymbol{x}})$	= local normal velocity
V	= $n \times n$ unitary matrix composed of the eigenvectors of (A^TA)
$V(\lambda)$	= generalized cross-validation (GCV) function
$\boldsymbol{x}$	= unknown parameter matrix
$\bar{\boldsymbol{x}}$	= observer positions in the frame fixed to the undisturbed medium
$\boldsymbol{x}_{\text{reg}}$	= regularized solution
$\boldsymbol{y}$	= source position
γ_i	= generalized singular values, $i = 1, \ldots, n$
θ	= angle between $\boldsymbol{n}$ and $\hat{\boldsymbol{r}}$
λ	= regularization parameter
λ_{opt}	= optimal regularization parameter
ρ_0	= density of undisturbed medium
σ_g	= variance of additive noise unbiased with Gauss distribution
σ_i	= singular values, $i = 1, \ldots, n$
Ω_r	= $(\omega \times \hat{\boldsymbol{n}}) \cdot \hat{\boldsymbol{r}}$, ω is angular velocity of body
$\Box^2$	= D'Alembertian, $1/c_0^2\partial^2/\partial t^2 - \nabla^2$

Received April 13, 1995; presented as Paper 95-0180 at the AIAA 16th Aeroacoustics Conference, Munich, Germany, June 12–15, 1995; revision received Nov. 28, 1995; accepted for publication Nov. 28, 1995.

*Assistant Professor, Department of Jet Propulsion, No. 407.
†Professor, Department of Jet Propulsion, No. 407.

Introduction

OVER the past two decades, prediction and control of propeller/prop-fan noise have been the most important subjects in aeroacoustics. Many techniques including time domain methods and frequency domain methods have evolved. However, all of these methods require the steady aerodynamics of the propeller to be obtained from computational fluid dynamics (CFD) or experimental methods. When propeller aeroacoustic experiments are carried out in a finite size of anechoic chamber, only a finite number of measurements can be made. It is highly desirable for both theoretical and practical applications to develop a technique for the spatial transformation of sound field (STSF) so that a limited set of measurements can be extended to describe the complete acoustic field.

Most of the techniques for the reconstruction of an acoustic field are based on the Helmholtz' integral equation (HIE), which requires the measurement of pressure and particle velocity over a surface enclosing the source. The theory describing this method in acoustics was proceeded by the work in the field of optics developed by Parrent[1] and others. Ferris[2] showed how the far-field sound pressure could be predicted from the cross spectra measured over a surface enclosing the source in the near-field region. Shewell and Wolf[3] described the inverse diffraction of monochromatic (single-frequency) coherent wave fields that laid a basis of acoustic holography. Their plane-to-plane diffraction theory allows prediction of the field closer to the source than the measurement plane. However, evanescent waves that are of great importance in acoustics are not reconstructed. Williams and Maynard[4] introduced near-field acoustic holography (NAH) to remove this drawback, and the generalized NAH theory was later given by Maynard et al.[5]

Since then, the NAH technique has been greatly improved. The so-called STSF technique[6] applies NAH and the HIE to give a

cross-spectral description of the sound field. By doing so, the coherence and single-frequency restrictions in conventional implementations of NAH and HIE are avoided. Based on cross spectra measured over a planar surface close to the source under investigation, all parameters of the sound filed can be mapped over a three-dimensional region extending from the surface of source to infinity. The near field is predicted from the measured data using NAH, whereas the more distant field is calculated using HIE. The STSF technique has found many applications in many areas, such as in the automobile industry.[7]

For STSF, all previously published techniques[4–7] are limited to stationary sound sources. The basic aim of this paper is to develop an STSF method suitable for moving surfaces such as propellers. In this case, the governing equation is the Ffowcs Williams and Hawkings (FW-H) equation[8] with the quadrupole source term neglected. Since the blade surface velocity is fully specified, numerical inversion of Farassat's integral[11] allows the blade surface pressures to be obtained from the field pressures. Furthermore the whole sound field can be predicted with the reconstructed aerodynamic loading. The main difficulty is that the inverse problem is mathematically ill posed, which means that any small errors in observer data lead to very large solution errors unless stability constraints are imposed. This paper will demonstrate that the Tikhonov regularization method[13] is effective in solving the discrete ill-posed problem. Finally, a numerical example of a conventional propeller is presented to show the feasibility of the proposed method.

Propeller Noise Prediction in Free Space

The governing differential equation for the acoustic field used here is the FW-H equation.[8] The quadrupole noise term in this equation is only important when the blade tip Mach number is transonic or supersonic[9] and so can be neglected for a subsonic moving surface. Let $f(\boldsymbol{y}, \tau) = 0$ describe the surface of the blade. It is assumed that $f > 0$ outside the body. The FW-H equation can be written as

$$\Box^2 p' = \frac{\partial}{\partial t}[\rho_0 v_n |\nabla f| \delta(f)] - \frac{\partial}{\partial x_i}[l_i |\nabla f| \delta(f)] \tag{1}$$

The two terms on the right-hand side of Eq. (1) are known as the thickness and loading sources, respectively.

Farassat[10,11] has given several integral solutions to Eq. (1). Here we assume the aerodynamic loading on the surface of the propeller is steady and Farassat's formula 1-A[11] can be used in the form

$$4\pi p'_L(\bar{\boldsymbol{x}}, t) = \frac{1}{c_0}\int_{f=0}\left[\frac{\dot{p}\cos\bar{\theta} + p\Omega_r}{r(1-M_r)^2}\right]_{\text{ret}} \mathrm{d}S + \int_{f=0}\left[\frac{p(\cos\bar{\theta} - M_n)}{r^2(1-M_r)^2}\right]_{\text{ret}} \mathrm{d}S + \frac{1}{c_0}\int_{f=0}\left[\frac{p\cos\bar{\theta}\left(r\dot{M}_i\hat{r}_i + c_0 M_r - c_0 M^2\right)}{r^2(1-M_r)^3}\right]_{\text{ret}} \mathrm{d}S \tag{2}$$

$$4\pi p'_T(\bar{\boldsymbol{x}}, t) = \int_{f=0}\left[\frac{\rho_0 v_n\left(r\dot{M}_i\hat{r}_i + c_0 M_r - c_0 M^2\right)}{r^2(1-M_r)^3}\right]_{\text{ret}} \mathrm{d}S \tag{3}$$

$$p'(\bar{\boldsymbol{x}}, t) = p'_L(\bar{\boldsymbol{x}}, t) + p'_T(\bar{\boldsymbol{x}}, t) \tag{4}$$

To apply Eqs. (2–4), the moving surface is divided into panels, and the integrands are calculated for each panel and are finally summed over all panels. For a body approximated by N panels, the discrete form of Eq. (4) is

$$4\pi p'(\bar{\boldsymbol{x}}, t) = \sum_{j=1}^{N} p_j \int_j K_p \,\mathrm{d}S + \sum_{j=1}^{N} v_{nj} \int_j K_{v_n} \,\mathrm{d}S \tag{5}$$

where

$$K_p = \left[\frac{\Omega_r(1-M_r) + \dot{M}_r\cos\bar{\theta}}{c_0 r(1-M_r)^3} + \frac{(1-M^2)\cos\bar{\theta} - (1-M_r)M_n}{r^2(1-M_r)^3}\right]_{\text{ret}}$$

$$K_{v_n} = \rho_0\left[\frac{\dot{M}_r}{r(1-M_r)^3} + \frac{c_0\left(M_r - M^2\right)}{r^2(1-M_r)^3}\right]_{\text{ret}}$$

The direct problem requires aerodynamic data as input that is usually obtained via CFD or experimental methods. Once the boundary condition has been specified, the radiated sound field is unique, which implies that the direct problem is well posed.

Pressure Reconstruction on the Blade Surface

To determine the pressure distribution on the surface of a propeller from a finite number of sound field pressure measurements, the integral equation (5) must be rearranged.

Assume $M(M \geq N)$ is the number of field data points so that Eq. (5) can be written in matrix form as

$$[4\pi p'] = [A][p] + [B][v_n] \tag{6}$$

where $A_j = \int_j K_p \,\mathrm{d}s$, $B_j = \int_j K_{v_n} \,\mathrm{d}s$, and $j = 1, \ldots, N$.

Since the blade surface velocity is fully specified, the steady pressure distribution p can be derived from Eq. (6):

$$[p] = [A]^{-1}\{[4\pi p'] - [B][v_n]\} = [A]^{-1}[4\pi p'_L] \tag{7}$$

The sound pressure spectrum can be obtained by using the Fourier transform,

$$4\pi p'_{Ln}(\bar{\boldsymbol{x}}) = \frac{\omega}{2\pi}\int_0^{2\pi/\omega} p'_L(\bar{\boldsymbol{x}}, t)\cdot\exp(in\omega t)\,\mathrm{d}t \tag{8}$$

which can be discretized as

$$4\pi p'_{Ln}(\bar{\boldsymbol{x}}) = \frac{1}{K}\sum_{k=0}^{K-1} p'_L(\bar{\boldsymbol{x}}, k\Delta)\cdot\exp(2\pi ink/K) \tag{9}$$

where $t = k\Delta$, $k = 0, 1, \ldots, K-1$, $\Delta = T/K$.

Using these results the inversion can be carried out in the frequency domain.

Analysis and Solution of the Ill-Posed Problem

We can write Eq. (7) or Eq. (9) in the abstract form

$$A\boldsymbol{x} = \boldsymbol{b} \tag{10}$$

where A is an $m \times n$ rectangular matrix with $m \geq n$, and $\boldsymbol{b} = \bar{\boldsymbol{b}} + \boldsymbol{e}$.

In general, the inverse problem is ill posed. By Hadamard's definition, a problem is well posed if the solution exists, is unique, and depends continuously on the data; otherwise, it is ill posed. For most physical cases, errors and noise are inevitable in experimental data while an ill-posed inverse problem is very sensitive to the exact formulation. Small errors in the data can lead to large errors in the solution unless suitable stabilizing constraints are imposed, i.e., unless additional a priori knowledge can be introduced. An interesting and important aspect of discrete ill-posed problems is that the ill-conditioning does not prevent a meaningful approximate solution from being computed. Rather, the ill-conditioning implies that standard methods in linear algebra for solving Eq. (10), such as Gauss elimination, LU, Cholesky, or QR factorization, cannot be used in a straightforward manner. Instead, more sophisticated methods must be applied to ensure the computation of a meaningful solution.

The least-squares (LS) estimate of $\boldsymbol{x}$ is

$$\boldsymbol{x} = (A^T A)^{-1} A^T \boldsymbol{b} \tag{11}$$

if $(A^T A)^{-1}$ exists. The matrix inversion will be numerically unstable if any of the eigenvalues of the matrix $(A^T A)$ are close to zero.

Hence, in the conventional LS inverse filtering, an extra term $\lambda^2 \boldsymbol{I}$ is often added to $(A^T A)$ to make the inversion stable. The term λ^2 is a white noise factor, and $\boldsymbol{I}$ has a dimension of $n \times n$. This is the essential goal of the Tikhonov regularization solution,[13,14] which can be defined as the following stabilized LS estimate:

$$\boldsymbol{x}_{\text{reg}} = (A^T A + \lambda^2 \boldsymbol{I})^{-1} A^T \boldsymbol{b} \tag{12}$$

The A matrix can be decomposed into a product of three matrices by singular value decomposition[12]:

$$A = U \begin{bmatrix} \Sigma \\ 0 \end{bmatrix} V^T \tag{13}$$

where superscript T denotes the complex conjugate transposed. The matrix

$$\begin{bmatrix} \Sigma \\ 0 \end{bmatrix}$$

is a rectangular diagonal matrix with the real nonnegative singular values series arranged in descending order of magnitude, that is,

$$\Sigma = \text{diag}[\sigma_1, \ldots, \sigma_n] \tag{14}$$

where $\sigma_1 \geq \cdots \geq \sigma_n \geq 0$. Substituting Eq. (13) into Eq. (12), one obtains

$$\boldsymbol{x}_{\text{reg}} = V \,\text{diag}\left(\frac{\sigma_i}{\sigma_i^2 + \lambda_2}\right) U^T \boldsymbol{b} \tag{15}$$

The essence of this method is that the singular value decomposition (SVD) has been combined with the Tikhonov regularization method by replacing the element σ_i in the

$$\begin{bmatrix} \Sigma \\ 0 \end{bmatrix}^{-1}$$

matrix by the element

$$\frac{\sigma_i}{\sigma_i^2 + \lambda^2}$$

It now becomes clear how λ can eliminate the problem of matrix singularities: even if $\sigma_i \to 0$, division by zero does not occur.

Following Jackson,[15] the resolution matrix in model space can be written as

$$\boldsymbol{R} = V \,\text{diag}\left(\frac{\sigma_i^2}{\sigma_i^2 + \lambda^2}\right) V^T \tag{16}$$

If $\boldsymbol{R}$ is the identity matrix $\boldsymbol{I}$, resolution is perfect and the particular solution is equal to the true solution. If the row vectors of $\boldsymbol{R}$ have components spread around the diagonal (with low values elsewhere), the particular solution represents a smoothed solution over the spread.

The trace of $\boldsymbol{R}$, which is a measure of resolution in model space, is

$$\boldsymbol{R}_{\text{tr}} = \sum_{i=1}^{n} \frac{\sigma_i^2}{\sigma_i^2 + \lambda^2}$$

which is clearly smaller than n. Thus the introduction of λ^2 will stabilize the solution by sacrificing the resolution.

In addition, there is an underlying assumption of using the Tikhonov regularization method which is that the errors in the right-hand sid are unbiased and their covariance matrix is proportional to the identity matrix. If the latter condition is not satisfied, one should incorporate the additional information and rescale the problem or use a regularized version of the general Gauss–Markov linear model.[16] Furthermore, no matter which method is used, the so-called discrete Picard condition (DPC) must be satisfied,[17] which states that the unperturbed right-hand side $\bar{\boldsymbol{b}}$ in a discrete ill-posed problem with regularization matrix L satisfies the DPC if the Fourier coefficients $|\boldsymbol{u}_i^T \bar{\boldsymbol{b}}|$ on the average decay to zero faster than the generalized singular value γ_i. For the Tikhonov regularization method, we have $L = \boldsymbol{I}$ and $\gamma_i = \sigma_i$. The DPC plays a important role in analyzing the discrete ill-posed problem.

Although the Tikhonov regularization method seems very useful, it is a nontrivial matter to choose a suitable value of the regularization parameter λ, which controls the degree of smoothness of the solution. Here we use the generalized cross-validation (GCV) method[18] that is based on the philosophy that if an arbitrary element b_i is left out, then the corresponding regularized solution should predict this observation well, and the choice of regularization parameter should be independent of an orthogonal transformation of $\boldsymbol{b}$.

The basic formula of GCV can be written as

$$V(\lambda) = \frac{\|[\boldsymbol{I} - \boldsymbol{P}(\lambda)]\|^2}{\{\text{tr}[\boldsymbol{I} - \boldsymbol{P}(\lambda)]\}^2}$$

in the case of the Tikhonov regularization,

$$\boldsymbol{P}(\lambda) = A(A^T A + \lambda^2 \boldsymbol{I})^{-1} A^T$$

Bringing Eq. (13) into $\boldsymbol{P}(\lambda)$ and using

$$z = U^T \boldsymbol{b}$$

we can write $V(\lambda)$ as

$$V(\lambda) = \frac{\|\boldsymbol{b}\|^2 - \|z\|^2 + \sum_{i=1}^{n} \left[\lambda^2 / \left(\sigma_i^2 + \lambda^2\right)\right]^2 z_i^2}{\left\{m - n + \sum_{i=1}^{n} \left[\lambda^2 / \left(\sigma_i^2 + \lambda^2\right)\right]\right\}^2} \tag{17}$$

Once the SVD of $\boldsymbol{P}(\lambda)$ is computed, the optimum value of λ_{opt} is determined by minimization of $V(\lambda)$. Equation (17) indicates that, for most problems, $\sigma_n \leq \lambda_{\text{opt}} \leq \sigma_1$. After λ_{opt} is chosen, the corresponding $\boldsymbol{x}$ is calculated using Eq. (15).

Besides the GCV criterion, the L-curve criterion is a good alternative for choosing an optimal regularization parameter, which can be referred to Refs. 19–21.

Results and Discussion

To test the feasibility of preceding proposed method, a conventional propeller is used as the numerical example and its main parameters are as follows: number of blades = 3, diameter = 2.49 m, flight speed $V_f = 82.78$ m/s, rotating speed = 2200 rpm, $c_0 = 339.14$ m/s, and $\rho_0 = 1.19$ kg/m^3.

The test consists of the following four procedures:

1) A panel theory[22] is used to calculate aerodynamic blade surface pressures.

2) The sound field is predicted using Eq. (5).

3) The blade surface pressures are reconstructed using Eq. (9).

4) The spatial transformation of the discrete sound field is obtained using Eq. (5).

Although the inversion can be performed in the time domain using Eq. (8), it consumes larger computer memory and CPU time than that of using Eq. (9) (for details see Ref. 20).

Figure 1 gives the observer positions in a ground-fixed frame $(R_{\text{ob}}, \theta, Z)$. The origin of this frame (O) is at the propeller center at time $t = 0$. The propeller disk is in the (R_{ob}, θ) plane and the Z axis coincides with the propeller axis (positive direction in the flight direction). In the test problem, 24 observer locations have been used for the inversion procedure. Note that the observer positions can be evenly or randomly distributed in space (in the far or near field) as long as they are not on the axis of the propeller where the discrete sound field is zero. An equally spaced grid reduces the

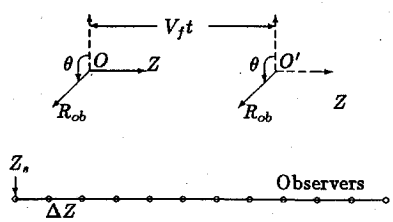

Fig. 1 Flight propeller and stationary observers in the ground-fixed frame $(R_{\text{ob}}, \theta, Z)$.

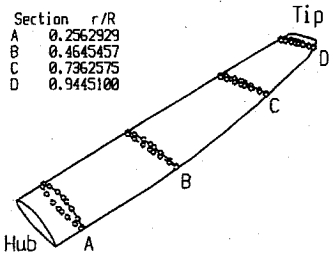

Fig. 2 Grid points generated on blade surface.

condition number of the matrix A, which makes the inversion procedure easier,[20] and the generated grid points are shown in Fig. 2 (64 points). For each observer location, the first 12 harmonics are used for inversion, and then A is an overdetermined matrix of dimension 288×64.

To simulate $p'(\bar{x}, t)$ containing measurement errors, random errors are added to the exact sound pressures as

$$[p'(\bar{x}, t)]_m = [p'(\bar{x}, t)]_d + e$$

where $[p'(x, t)]_m$ is the simulated sound pressures, $[p'(x, t)]_d$ is the exact sound pressures, and e is the perturbation vector that has zero mean and covariance matrix $\sigma_g^2 = I_m$. The signal-to-noise ratio is defined by

$$\frac{S}{N} = \left[\frac{1}{m}\frac{\|[p'(\bar{x}, t)]_d\|^2}{\sigma_g^2}\right]^{\frac{1}{2}}$$

Since $[p'(\bar{x}, t)]_d$ is fully specified, S/N depends inversely on σ_g, which means $S/N \to \infty$ when $\sigma_g \to 0$. However, S/N has an upper limit because $[p'(\bar{x}, t)]_d$, includes round-off errors, so that $S/N = \infty$ in the following results represents a finite number that is dependent on the computer being used for the calculation.

We first analyze whether the discrete Picard conditions have been satisfied for several different S/N levels as shown in Fig. 3. For these test cases, the condition number (σ_1/σ_n) is as large as 10^7, which means matrix A is ill conditioned. It is obvious that the DPC has been satisfied very well for $S/N = \infty$ because the data have not been contaminated by additive noise, although eventually, for about $i > 55$, and $\sigma_{55} \approx 5 \times 10^{-6}$, both the singular values σ_i and the Fourier coefficients $u_i^T b$ become gradually dominated by rounding errors. For the noisy test problems ($S/N = 76.5, 7.65, 0.765$), the Fourier coefficients become dominated by the perturbation for i much smaller than before. Even then, in the left part of the curve the Fourier coefficients still decay faster than the singular values, indicating that the unperturbed right-hand side satisfies the DPC, although the i that can satisfy the DPC decreases with S/N, i.e., $S/N = 0.765$, $i < 3$, and $\sigma_3 = 11.4$. This means that it is still possible to dampen the components for which the perturbation dominates with the regularization method by degrading the resolution.

For the Tikhonov regularization method, the optimal regularization parameters chosen by the GCV criterion for a wide range S/N levels are shown in Fig. 4. It is seen that λ_{opt} decreases gradually with increasing S/N for $S/N < 10^7$. For example, if $S/N = 0.765$, then $\lambda \approx 10.8$, and if $S/N = 7.65 \times 10^6$, then $\lambda \approx 4.9 \times 10^{-6}$, which is very close to the DPC analysis given earlier. Moreover, the almost constant values of λ_{opt} for $S/N > 10^7$ show that these test cases are dominated by rounding errors. Consequently, the maximum S/N level is around 10^7 for this test problem. Furthermore, although the introduction of λ stabilizes the solution, Fig. 5 shows that the resolutions R_{tr} depend inversely on the regularization parameter λ. An interesting and important point is that the value of R_{tr} corresponding to the λ_{opt} chosen by the GCV criterion is very close to the value of i that satisfies the DPC. This illustrates that an optimal regularization parameter chosen by GCV or any other criterion should satisfy the DPC.

Once the optimal regularization parameter has been chosen, the blade pressures can be reconstructed. Several reconstruction results compared with exact results are shown in Fig. 6. For the case of $S/N = \infty$, all of the reconstructed results agree well with the exact

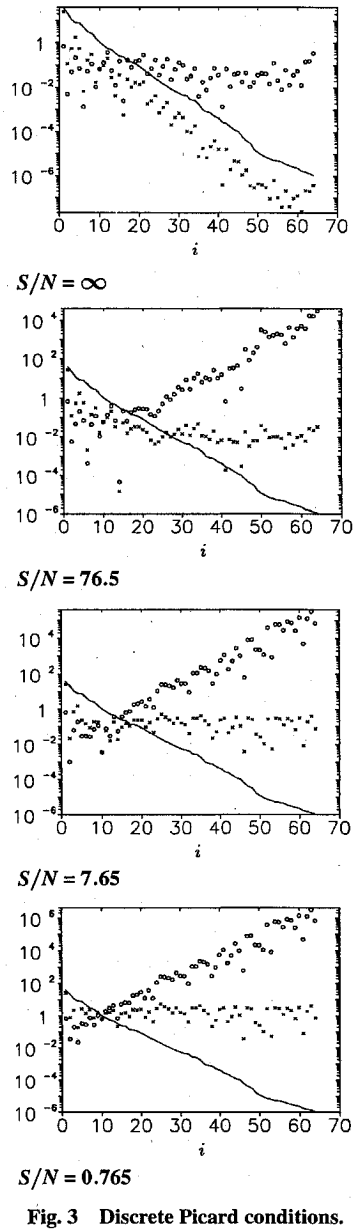

Fig. 3 Discrete Picard conditions.

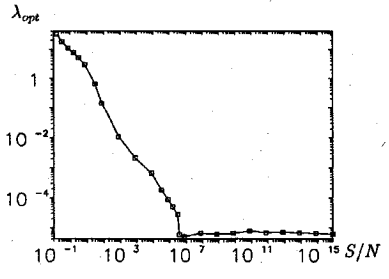

Fig. 4 Optimal regularization parameters λ_{opt} varying with S/N.

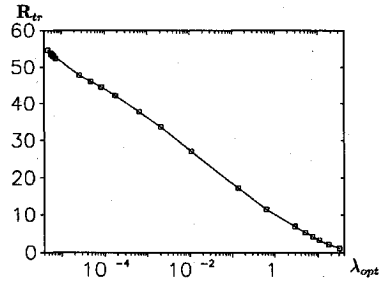

Fig. 5 Trace of R varying with the optimal regularization parameters λ_{opt}.

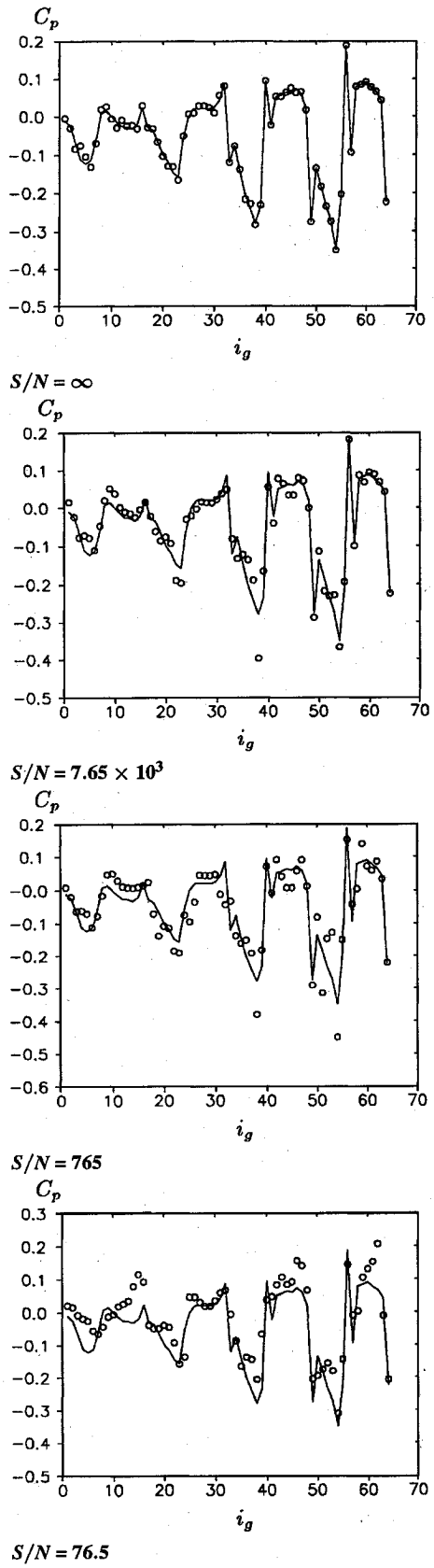

Fig. 6 Reconstructed pressure distribution.

solution except some errors that occur near the hub of blade. This can be explained by the fact that the discrete sound filed of the propeller is dominated by the contribution from the tip region. However, the reconstruction accuracy decreases rapidly with decreasing S/N. When the S/N is reduced to 76.5, the reconstruction error becomes unacceptably large.

The whole sound field can be predicted from the reconstructed blade pressures. The direct sound field is shown in Fig. 7, and the

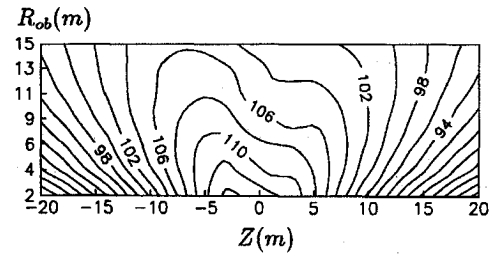

Fig. 7 Direct sound field.

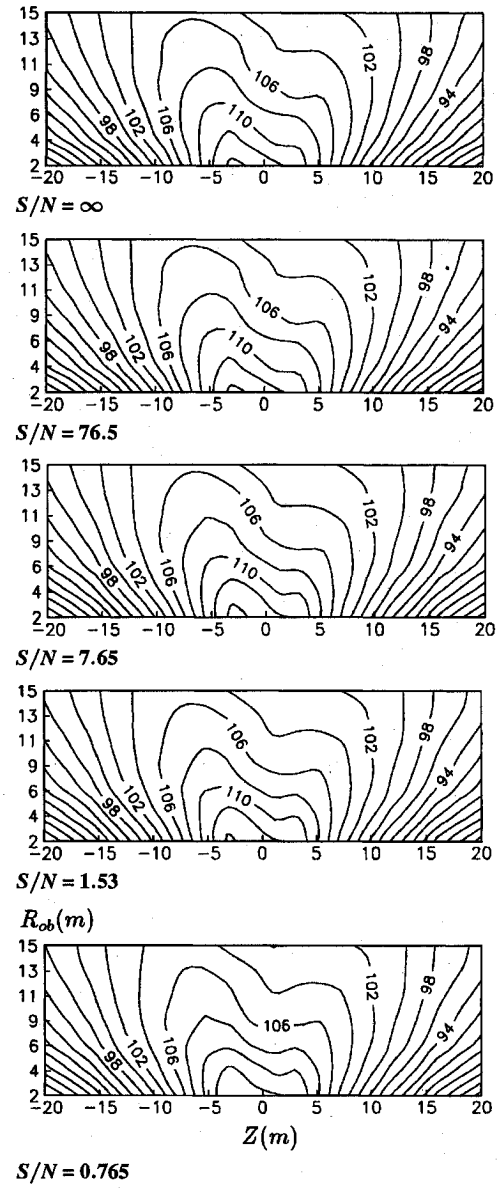

Fig. 8 Extrapolated sound field.

STSF results for different S/N are shown in Fig. 8. We can see that the accuracy of the STSF decreases very slowly with increasing S/N. If $S/N > 1$, the STSF results can be guaranteed with high accuracy. These results show that the reconstruction can be considered as an intermediary for the practical extrapolation of the acoustic field from propellers.

Concluding Remarks

A technique for the spatial transformation of discrete sound fields from propellers has been developed that is based on solving the FW-H equation with the quadrupole source term neglected. The main difficulty of the proposed technique is that this problem is mathematically illposed. The singular value decomposition

technique combined with the Tikhonov regularization method has been shown to be a powerful tool for stabilizing the solutions, and the generalized cross-validation criterion is successful in choosing the optimal regularization parameters.

The feasibility of the method is tested for one numerical example for a conventional propeller of which aerodynamics are computed by means of a panel method. The computed radiation is used to reconstruct the blade surface pressures. Numerical results show that small errors in observer data lead to large reconstruction errors. Even then, the reconstruction is capable of predicting the field accurately if the signal-to-noise ratio $S/N > 1$. This means that the reconstruction is inaccurate in the presence of measurement noise (error) but can be used as a vehicle for field extrapolation.

Although the numerical results presented in this paper are limited to a conventional propeller, the technique can be extended to any subsonic moving surface that is worthy of further research.

Acknowledgments

This work is supported by the National Defence Scientific Foundation of China. The authors are grateful to Xiao-feng Sun and Peng Shan for their continuous assistance and fruitful discussions.

References

[1]Parrent, G. B., "On the Propagation of Mutual Coherence," *Journal of the Optical Society of America*, Vol. 49, Nos. 7, 8, 1959, pp. 787–793.

[2]Ferris, H. G., "Farfield Radiation Pattern of a Noise Source from Nearfield Measurements," *Journal of the Acoustical Society of America*, Vol. 36, No. 8, 1964, pp. 1597, 1598.

[3]Shewell, J. R., and Wolf, E., "Inverse Diffraction and a New Reciprocity Theorem," *Journal of the Optical Society of America*, Vol. 58, No. 12, 1968, pp. 1596–1603.

[4]Williams, E. G., and Maynard, J. D., "Holographic Imaging Without the Wavelength Resolution Limit," *Physical Review Letters*, Vol. 45, No. 7, 1980, pp. 554–557.

[5]Maynard, J. D., Williams, E. G., and Lee, Y., "Nearfield Acoustic Holography: I. Theory of Generalized Holography and the Development of NAH," *Journal of the Acoustical Society of America*, Vol. 78, No. 4, 1985, pp. 1395–1413.

[6]Hald, J., "STSF—A Unique Technique for Scan-Based Near-Field Acoustic Holography Without Restrictions on Coherence," *Technical Review*, BV 0035-11, B&K, Naerum, Denmark, 1989.

[7]Nakamura, M., Komine, T., Tsuchiya, M., and Hald, J., "Measurement of Aerodynamic Noise Using STSF," BO 0392-11, B&K, Naerum, Denmark, 1994.

[8]Ffowcs Williams, J. E., and Hawkings, D. L., "Sound Generated by Turbulence and Surfaces in Arbitrary Motion," *Philosophical Transactions of the Royal Society of London*, Vol. 264A, 1969, pp. 321–342.

[9]Hanson, D. B., and Fink, M. R., "The Importance of Quadrupole Sources in Prediction of Transonic Tip Propeller Noise," *Journal of Sound and Vibration*, Vol. 62, No. 1, 1979, pp. 19–48.

[10]Farassat, F., "Linear Acoustic Formulas for Calculation of Rotating Blade Noise," *AIAA Journal*, Vol. 19, No. 9, 1981, pp. 1122–1130.

[11]Farassat, F., "The Evolution of Methods for Noise Prediction of High Speed Rotors and Propellers in the Time Domain," *Recent Advances in Aeroacoustics*, edited by A. Krothapalli and C. A. Smith, Springer–Verlag, New York, 1986, pp. 129–147.

[12]Golub, G. H., and Kahan, W., "Calculating the Singular Value Decomposition and Pseudo-Inverse of a Matrix," *SIAM Journal on Numerical Analysis*, Vol. 2, No. 2, 1965, pp. 205–224.

[13]Tikhonov, A. N., "Solution of Incorrectly Formulated Problems and the Regularization Method," *Doklady Akademii Nauk SSSR*, Vol. 151, 1963, pp. 501–504; also *Soviet Mathematics Doklady*, Vol. 4, 1963, pp. 1035–1038.

[14]Tikhonov, A. N., and Arsenin, V. Y., *Solutions of Ill-Posed Problems*, Wiley, NewYork, 1977.

[15]Jackson, D. D., "Interpretation of Inaccurate, Insufficient and Inconsistent Data," *Geophysical Journal of Royal Astronomical Society*, Vol. 28, No. 2, 1972, pp. 97–109.

[16]Zha, H., and Hansen, P. C., "Regularization and the General Gauss-Markov Linear Model," *Mathematics of Computation*, Vol. 55, No. 192, 1990, pp. 613–624.

[17]Hansen, P. C., "The Discrete Picard Condition for Discrete Ill-Posed Problems," *BIT*, Vol. 30, No. 4, 1990, pp. 658–672.

[18]Bates, D. M., Lindstrom, M. J., Wahba, G., and Yandell, B., "GCVPACK-Routines for Generalized Cross Validation," *Communications in Statistics Simulation and Computation*, Vol. 16, No. 1, 1987, pp. 263–297.

[19]Hansen, P. C., "Analysis of Discrete Ill-Posed Problems by Means of L-Curve," *SIAM Review*, Vol. 34, No. 4, 1992, pp. 561–580.

[20]Li, X. D., "A New Kind of Inverse Problem in Aerodynamics and Aeroacoustics," Ph.D. Dissertation, Dept. of Jet Propulsion, Beijing Univ. of Aeronautics and Astronautics, Beijing, PRC, May 1995.

[21]Li, X. D., and Zhou, S., "An Inversion Model for Subsonic Moving Sound Source Reconstruction," AIAA Paper 95-0120, June 1995.

[22]Pan, J. Y., and Qian, H. D., "Aerodynamic Design of Propeller by Numerical Optimization," *Journal of Aerospace Power*, Vol. 6, No. 4, 1991, pp. 300–304.